Boundary-Layer Meteorology (2006)
DOI 10.1007/s10546-005-9028-2

SURFACE FLUXES AND CHARACTERISTICS OF DRYING SEMI-ARID TERRAIN IN WEST AFRICA

D. SCHÜTTEMEYER[1,2,*], A. F. MOENE[1], A. A. M. HOLTSLAG[1], H. A. R. DE BRUIN[1] and N. VAN DE GIESEN[2,**]

[1]*Meteorology and Air Quality Group, Wageningen University, Duivendaal 2, 6701 AP Wageningen, The Netherlands;* [2]*Centre for Development Research, University of Bonn, D-53113 Bonn, Germany*

(Received in final form 20 September 2005)

Abstract. This study examines the seasonal cycle of the components of the surface energy balance in the Volta basin in West Africa as part of the GLOWA-Volta project. The regional climate is characterized by a strong north–south gradient of mean annual rainfall and the occurrence of pronounced dry and wet seasons within one annual cycle, causing a strong seasonal variation in the natural vegetation cover. The observations are conducted with a combined system, consisting of a Large Aperture Scintillometer (LAS) for areally averaged sensible heat flux, radiometers and sensors for soil heat flux. For comparisons the eddy-covariance (EC) method providing the fluxes of momentum, sensible and latent heat is utilized as well. The measurements of a seasonal cycle in 2002/2003 were gathered including the rapid wet-to-dry transition after the wet season at two locations in Ghana, one in the humid tropical southern region and one in the northern region. A direct comparison and the energy balance closure of the two methods are investigated for daytime and nighttime separately. An attempt is made to understand and explain the differences between the two methods and the closure of energy budget found for these. It is found that the two systems correspond well during daytime. During nighttime the LAS seems to perform more realistically than the EC system. Considering the fact that a LAS system is much easier to use in the climate conditions of the Volta basin, it is concluded that the LAS approach is very suitable in this type of climate conditions. Surface conductances are estimated by rearranging the Penman–Monteith equation and compared to a Jarvis-type model optimised for savannah conditions. It is found that temperature dependence should be included in the conductance formulation in contrast to earlier findings. Based on the findings the gathered dataset can be used for further model studies of the climate and environment of West Africa.

Keywords: Eddy covariance, Energy balance closure, Scintillometry, Semi-arid, Surface conductance, West Africa.

* E-mail: dirk.schuettemeyer@wur.nl
** Present address: University of Technology, Delft, The Netherlands.

1. Introduction

It is widely recognized that the parameterisation of land surface processes, in particular the way energy is partitioned at the earth's surface, significantly affects the performance of regional weather and climate models. Since the parameterisation schemes in those models are essentially semi-empirically, there is a strong need to validate and to calibrate these schemes with experimental data. During the last decade large efforts have been made to establish accurate micrometeorological measurements of energy flux components at longer time scales to tackle that need, see for example EFEDA (Bolle et al., 1993) or FLUXNET (Baldocchi et al., 2001). However, there still is a lack of data for numerous ecosystems like the semi-arid regions in West Africa. This is important, because nearly one-fifth of the world's population lives in semi-arid regions covered with savannah type vegetation (Solbrig et al., 1996) and those regions, especially in West Africa, have been and will be subjected to pressure resulting from human activities. Furthermore, recent research has revealed that the current parameterisation schemes applied to the landscapes in West Africa require improvements; see for instance the African Monsoon Multidisciplinary Analyses (AMMA) project (http://medias.obs-mip.fr/amma).

The main characteristics in the West African landscape are humid tropical regions like the equatorial forests in the South, an intermediate zone with semi-humid areas such as the Guinea savannah and a northern region with mainly fallow savannah.

In the past, several projects have been performed yielding information on energy balance flux components in the more northern Sahel region like SEBEX (Wallace et al., 1992) with a focus on the annual cycle. Another example is HAPEX-SAHEL, which took place in 1992 for three months (Goutorbe et al., 1994). Verhoef et al. (1996a) discussed various influences like water vapour pressure deficit (VPD) and soil water content on the surface fluxes in this context.

For the more southern region including the Volta basin there is still a lack of data. The Volta basin is located in the intermediate zone and the southern part of West Africa. It comprises an area of about 400,000 km^2 and is considered as one of the benchmark watersheds for Africa (http://www.cgiar.org/iwmi/challenge-program). The present study describes measurements, which are part of long-term observations of the water and energy balance in Ghana in the Volta basin. This is done in the context of the GLOWA-Volta project (Global Change in the Hydrological cycle). The GLOWA-Volta Project, 'Sustainable Use of Water Resources: Intensified Land Use, Rainfall Variability, and Water Demands in the Volta Basin', has the goal of creating a scientifically sound decision-support system (DSS) for the assessment, development and sustainable use of water resources by means of an integrated model of the basin (Van de Giesen et al., 2001).

We regard turbulent energy fluxes (sensible and latent heat) as key components of that integrated model and since a model is usually only as accurate as the measurements used for its validation, one of the first steps is to analyse the measurements made. Certain techniques exist to measure turbulent energy fluxes as the two main components of the energy balance at the land surface. For the above-mentioned studies in the more northern region only standard methods suitable for homogenous surface (point observations) were used. Unfortunately, the climatic and environmental conditions in West Africa are not favourable to apply standard methods of observation. For instance, the savannah surface type is spatially inhomogeneous and its structure changes seasonally due to the pronounced existence of dry and wet periods. For that reason, there is a need for non-standard methods of observation such as the scintillometry for example proposed by De Bruin et al. (1995), which yield spatially averaged measurements of the energy balance term and which are suitable for long-term operational application in the West African landscape and climate.

Therefore, it is the objective of this study to investigate the applicability of a large aperture scintillometer (LAS) to determine the spatially averaged flux of sensible heat and, indirectly, the spatially averaged evaporation. The advantages of the LAS technique are that the areally averaged sensible heat flux can be obtained (up to 5000 m), and its robustness, which makes it suitable for long-term measurements in that kind of environment. For this purpose three test sites have been equipped with LAS along the climatic north–south gradient. The first focus in this study is on the applicability of the LAS in comparison with the eddy-covariance (EC) method. The agreement between both methods should also increase the confidence in the gathered data for further applications.

With this background a second focus is on analysing the conservation of energy. The conservation of energy is usually expressed as energy balance closure, which can be formulated as follows

$$R_{\mathrm{n}} = H + LE + G, \qquad (1)$$

R_{n} is net radiation, H is sensible heat flux, L the latent heat of vaporization, E the moisture flux and G is the soil heat flux. Theoretically the conservation of energy requires instantaneous closure for day and nighttime. In practice energy balance closure can be biased up to 30% during daytime, during nighttime even higher (Wilson et al., 2002), which normally goes along with a negative bias. In many situations the closure is enhanced over homogenous terrain and short vegetation (Mahrt, 1998; Twine et al., 2000). The reasons for the nonclosure are manifold and not always known. General hypotheses state sampling errors, systematic bias in instrumentation, neglected energy sinks, loss of low and/or high frequency contributions to the turbulent flux and neglected advection of scalars (Wilson et al., 2002) as potential sources of errors. In many situations two terms of the energy balance (net radiation and soil heat flux) are point measurements, whereas the turbulent fluxes contain information from a larger area. Soil heat flux is often treated improperly, neglecting or underestimating heat storage between the soil heat flux plate and the surface. If it is not properly measured or adjusted it can cause errors up to $100\,W\,m^{-2}$ (Heusinkveld et al., 2004). Energy balance closure is also a common tool to test the quality of turbulent energy flux data (Foken and Wichura, 1996; Lamaud et al., 2001).

Furthermore there is a need for a better understanding of the processes that control evapotranspiration due to seasonal dynamics (Viterbo and Beljaars, 1995). Therefore, the third focus is on obtaining a better knowledge of the changes in surface conductance during the chosen time period. The surface conductance is estimated from Penman–Monteith equation (Monteith, 1981) and compared to a Jarvis-type model (Jarvis, 1976) based on the findings of Dolman (1993) and Huntingford et al. (1995), who optimised the model for savannah conditions. The concept of obtaining surface conductance from Penman–Monteith equation has the potential to model water vapour exchange (Harris et al., 2003) and evaluate evaporation rates correctly (Baldocchi et al., 2004), when conservation of energy is achieved. The relationship between the surface conductance and the driving variables (radiation, vapour pressure deficit, temperature and soil moisture) throughout the time of transition might help in evaluating and validating surface fluxes obtained by regional weather and climate models.

In summary the objectives of this study are:

- To analyse the available data in order to set-up a reference dataset, suitable for atmospheric and hydrological modelling studies.
- To evaluate the differences of turbulent energy fluxes between LAS and EC based measurements under different meteorological conditions and surface types within the context of the closure of the energy balance.
- To evaluate the concept of surface conductances with different surface types and changing meteorological situations.

The experimental set-up, including a site description as well as a description of the LAS and EC technique, is given in Section 2. Section 3 describes the comparison of LAS and EC derived turbulent fluxes. In Section 4, the evaluation of the energy balance closure is presented. Section 5 provides the evaluation of the surface conductance. Each of the different sections includes a discussion of the outcome at the test sites. Finally, the major conclusions are reviewed in Section 6.

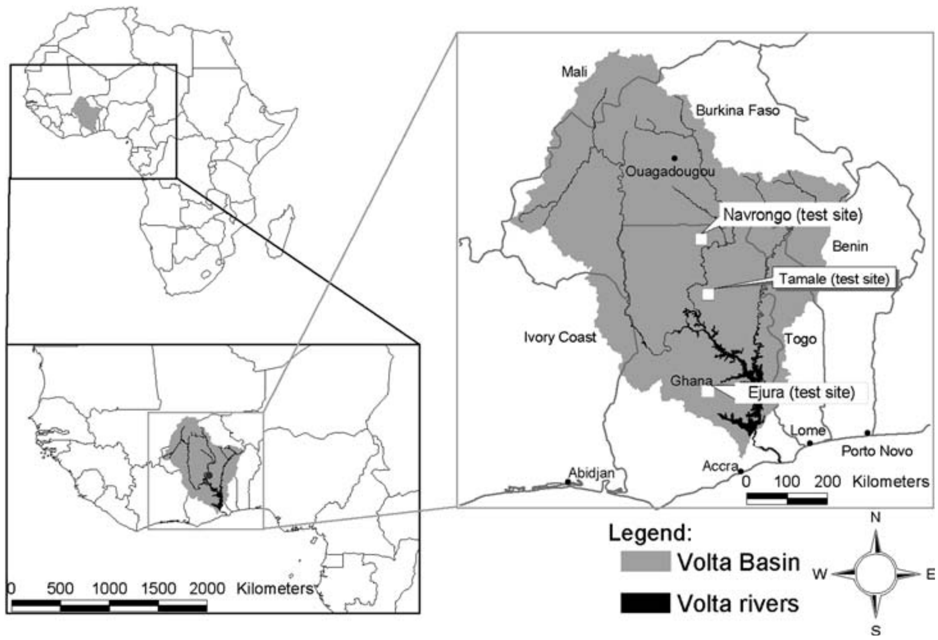

Figure 1. Location of experimental sites in Ghana within the GLOWA-Volta project (*Source:* Friesen, 2002).

2. Experimental Set-up and Observations

The climate system in West Africa is to a large extent controlled by the meridional movement of the intertropical convergence zone (ITCZ) during the year, the African Easterly Jet (AEJ) and pressure disturbances, which traverse from east to west across Africa (Burpee, 1972). They all act under the influence of the Hadley and Walker cell circulation. Those mechanisms lead to a pronounced wet and dry season during the year, of which the length depends on the actual latitude. During the time of the year when the wet period ends and the dry period starts (time of transition) the contrast between dry and moist air is probably more pronounced in time and space than anywhere else (Hólm et al., 2002). To account for the large variability during the year three test sites (Ejura (7°20′ N; 1°16′ W), Tamale (9°29′ N, 0°55′ W) and Navrongo (10°55′ N; 1°02′ W), Figure 1) were established in 2001 and are operational since then. The distance between the stations is about 100–200 km. Tamale is the central station. In the present study only data from Ejura and Tamale are analysed.

The annual mean temperature for the three sites varies from the most southern site Ejura (26.6 °C) over Tamale (27.8 °C) to Navrongo (28.2 °C). The annual mean precipitation, which is one of the driving forces for surface fluxes during the rainy period, varies from 900 to 1500 mm, where

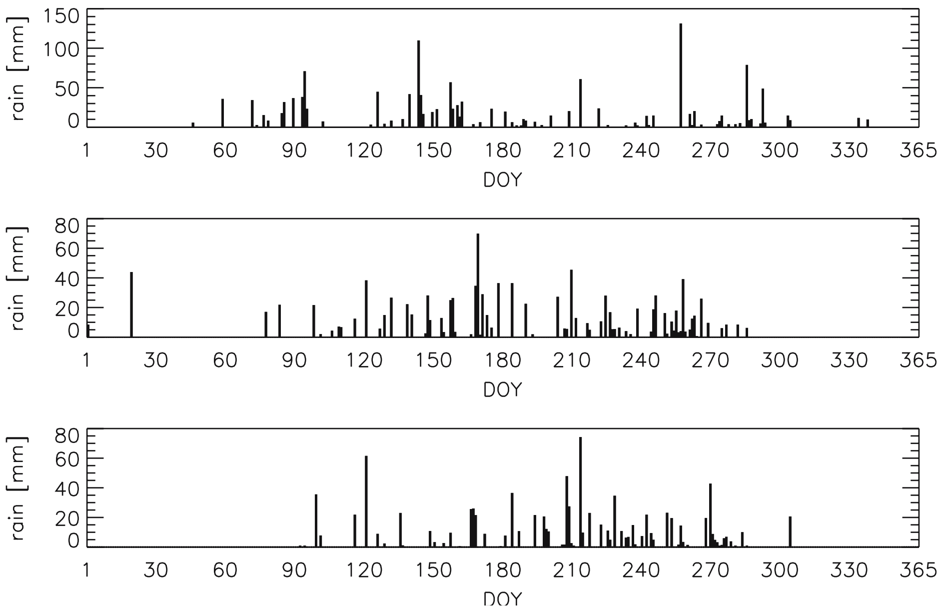

Figure 2. Daily sums of precipitation for the three test sites in Ejura (top), Tamale and Navrongo (bottom) in 2002.

more than 95% of the rain occurs during the rainy season. The mean annual rainfall at the sites is 1432 mm in Ejura, 1082 in Tamale, and 1043 mm in Navrongo (FAO, 1984, including data from 1930 to 1980). For 2002 there is a large difference in precipitation between the research sites. In Figure 2, daily sums of precipitation are shown for the test sites. For Ejura the yearly sum is 1420 mm, for Tamale it is 1065 mm and for Navrongo the total precipitation in 2002 is 890 mm.

The onset of the rainy period for 2002 is estimated as day of year (DOY) 74 for Ejura and DOY 118 for Tamale and Navrongo. The end is estimated as DOY 343 in Ejura and 290 for Tamale and Navrongo. This is done using the method of Kasei (1988). Malda (personal communication, 2002) analysed 40 years of precipitation for different stations in the Volta basin and found that the average onset for Ejura was DOY 78 with a standard deviation (SD) of 30 days. For Tamale it is DOY 115 (SD = 20) and Navrongo it is DOY 131 (SD = 19). Furthermore, no long-term trend could be found in his analyses. For the year 2002 the precipitation measurements and the analysis for the length of the season show that the total amount of rain and the length of the season are normal.

2.1. Meteorological measurements

All sites are equipped with automatic weather stations (AWS), which measure temperature, humidity and incoming solar radiation at a height of

2 m. Wind speed and direction are measured at 8 m height. Net radiation is measured directly and calibrations are wind speed corrected, due to the design of the NR-Lite (Kipp & Zonen). Additionally, surface observations are collected for soil heat flux at 0.035 m depth, precipitation, soil moisture at different depths, surface runoff using runoff plots and runoff at the outlet of each watershed using a flume or a weir. Type and brand of the instruments used are described in Table I.

All quantities are originally averaged for 10-min intervals. Data availability exceeds more than 90% for most of the measurements for all three sites during the year 2002.

The soil heat flux is measured by applying the method of Heusinkveld et al. (2004), whereby the conventional sensor is moved to a location just below the surface and compared to the analysis of the temperature wave propagation into the soil. This added 30–40% of soil heat flux at 0.035 m depth on average. Since soil temperature measurements are available in Tamale only, the method is applied there and should be of smaller importance in Ejura due to the fully vegetated surface (daytime: G=5–15% of R_n, night time: 50% of R_n) (Stull, 1988).

Soil heat flux plates should have a thermal conductivity similar to the soil, but the conductivity may vary due to changes in soil water content and temperature (Verhoef et al., 1996b). For Tamale there was no precipitation during the intensive observation period (IOP) and for Ejura this is valid for most of the time during the IOP, so the impact due to rainfall should be small.

Additionally sap flow, albedo, leaf area index and tree density data are collected. A survey for soil properties was done in Tamale and Ejura (Agyare, 2004). The following data on soil diagnostics were collected: horizon, texture, colour, structure, and presence of mottle, roots, and concretions from 0 to 0.15 m and 0.30–0.45 m depths.

Soil moisture deficit Θ (mm) is calculated by subtracting interpolated moisture contents from the maximum field capacity of the upper and lower soil type, which is calculated from the soil diagnostics based on the work of Schaap et al. (1998).

2.2. Flux measurements with Scintillometry

The LAS consists of a transmitter emitting electromagnetic radiation towards a receiver. The distance between both can be chosen up to 5000 m for a beam diameter of 0.15 m. In our case the distance varies between 1040 and 2420 m for the different sites. It is installed at a certain height above the surface. The emitted radiation is scattered by the turbulent medium in the path. The variance of intensity of received radiation is proportional to the structure parameter of the refractive index of air (C_n^2).

TABLE I
Instruments used for this study at the two test sites.

Variable	Location	Instrument
Air temperature	2 m	50Y Temperature and RH probe (Vaisala)
Relative humidity	2 m	50Y Temperature and RH probe (Vaisala)
Atmospheric pressure	Inbox	PTB101B Barometric Pressure Sensor (Vaisala)
Wind speed	8 m	A100R Anemometer (Vector Instruments)
Wind direction	8 m	Wind vane (Ecotech)
Net radiation	8 m	NR-LITE (Kipp & Zonen)
Downward solar radiation	2 m	SP-LITE (Kipp & Zonen)
Precipitation	2 m	Tipping bucket (Stelzner)
Sensible heat flux	10.0 m	CSAT3 Sonic anemometer (Tamale), Windmaster Pro (Gill) (Ejura),
	Site dependent	Large Aperture Scintillometer (LAS) (Manufactured by Wageningen Uni.)
Latent heat flux	10.0 m	CS7500 infrared hygrometer (Li-Cor) (Tamale), KH2O Krypton hygrometer (Campbell) (Ejura) Residual of the energy balance
Soil heat flux	0.035 m	HFP01 Heat Flux Plate (Hukseflux)
Soil temperature	Different depth	PT_{100}resistance thermometer (Manufactured by Wageningen Uni.)
Soil moisture	Different depth	TDR (Campbell) (Tamale), TDR (Delta-T) (Ejura)

At the wavelength used (940 nm) the refractive index mainly depends on temperature, so C_n^2 is mostly determined by temperature fluctuations (C_T^2),

$$C_T^2 = C_n^2 \frac{T^2}{A_T^2}\left(1 + \frac{A_q}{q}\frac{T}{A_T}\frac{c_p}{L}\beta^{-1}\right)^{-2}, \tag{2}$$

$$A_T = T\frac{\partial n}{\partial T} \text{ and } A_q = q\frac{\partial n}{\partial q},$$

which are both dependent on optical wavelength, pressure, temperature and humidity content. T is the mean air temperature and q is the mean specific humidity, c_p is the specific heat of air at constant pressure and L_v is the latent heat of vaporisation. The last factor at the right-hand-side of Equation (2) reflects an estimate of the influence of humidity on the refractive index (Wesely, 1976; Moene, 2003). Here ß is estimated as follows:

$$\beta = \frac{H_{LAS}}{R_n - G - H_{LAS}}. \tag{3}$$

Sensible heat flux is calculated from C_T^2 (Obukhov, 1960) by using the following expression: $H_{LAS} = \rho c_p u_* \Theta_*$ with u_* being the friction velocity and Θ_* being the temperature scale from Monin–Obukhov similarity theory (MOST). In this study a standard Businger–Dyer flux-profile relation is utilized for estimating u_* from wind speed and roughness length and H_{LAS} is calculated iteratively.

Stability functions proposed by Wyngaard (1973) are used for daytime values. For nighttime values we follow the formulation of De Bruin et al. (1993). Several tests are made for the use of different stability functions for day and nighttime situations. In general the results are steady and differ at most 10%, but especially during nighttime, the formulation of De Bruin gives the most reliable results. For a more detailed description of the LAS theory and its applications see for example De Bruin et al. (1995) and Meijninger et al. (2002).

The LAS at each site is installed on top of two opposite hills using towers with a minimum height of 5 m. The set-up with small differences in installation height of transmitter and receiver and changes in terrain height along the path implies that the height of the beam above the terrain varies along the path. The effective height is calculated using the method of Hartogensis et al. (2003) using the fact that the LAS signal is weighted towards the middle of the path. For both sites the orientation of the optical path is perpendicular to the prevailing wind direction (compare Figure 5).

Latent heat flux is calculated as a residual from the energy balance (Equation 1) with the help of the LAS measurements:

$$LE_{LAS} = R_n - H_{LAS} - G. \tag{4}$$

2.3. Intensive observation period 2002

Two test sites (Ejura, Tamale) were specifically instrumented with EC systems for an IOP. The period examined in Tamale started at DOY 307 and ended at DOY 349 in 2002. In Ejura it started at DOY 313 and ended at

DOY 28 in 2003. In Tamale additional measurements were taken for soil heat flux and soil temperature at different depths, skin temperature and additional radiation measurements.

Both periods include the transition from wet to dry, with an increase in temperature and vapour pressure deficit. Although the instrumentation of the sites in Ejura and Tamale differed (in terms of sonic anemometers, humidity sensor and sampling frequency), the processing of the EC data was identical for both sites (see Table I for an overview of the instrumentation). From the raw data (20 Hz sampling at Tamale, 10 Hz sampling at Ejura) half-hourly fluxes have been computed taking the following corrections into account:

- the raw data have been linearly detrended;
- the mean signal of the Krypton hygrometer has been adjusted using the humidity measurements of a slow-response sensor;
- axis rotation using the planar fit method, with planar fit angles determined on a daily basis (see Wilczak et al., 2001). The bias in the vertical velocity was set to zero;
- sonic temperatures were corrected for humidity (see Schotanus et al., 1983);
- the oxygen-sensitivity of the Krypton hygrometer was corrected for using the coefficients found by van Dijk et al. (2003);
- corrections for frequency response and path averaging according to Moore (1986);
- the Webb term for the water vapour flux has been taken into account (see Webb et al., 1980).

More details and software can be found at http://www.met.wau.nl/projects/jep.

2.4. Site description

The site in Ejura is characterized by dense vegetation and a short dry period. The landscape is hilly. The transmitter and the weather station are located in a cashew orchard. The receiver is located at the edge of a forest. The length of the path in between is about 2030 m. The weighted effective height of the LAS is 30.1 m. It is a heterogeneous terrain. The area between the transmitter and the receiver can roughly be divided into two parts. On the transmitter side the vegetation consists of cashew trees with a maximum height of 4 m and in between maize and grass with a maximum height of 2 m. On the receiver side there are bushes and trees and small swamps, but nearly no agriculture. The EC system was installed nearly in the middle of the path of the LAS, but still in the orchard.

The research site in Tamale is mainly characterized by grassland with scattered trees (cover about 15%), with a maximum height of 5–8 m and a large dry period. The landscape is slightly hilly. LAS transmitter and receiver are installed on two hills with a distance in between of about 2420 m. The weighted effective height of the LAS was estimated to 19.5 m. The automatic weather station is installed next to the receiver of the LAS. The EC system was installed nearly in the middle of the path.

2.5. Methods

In the current study data from the years 2002/2003 are analysed. The main focus is on the time of the year, when the monsoon period is ending and the time of transition starts. For all further evaluations the surface fluxes are calculated on a half-hourly basis. All other measurements are also averaged on that basis. The analyses are made with the background of dividing into daytime and nighttime values to overcome the problem of overestimating positive fluxes during the day and underestimating negative fluxes at night (Mahrt, 1998). Another reason is the use of different stability functions to calculate sensible heat flux from LAS measurements during unstable and stable situations. To divide into daytime and nighttime a simple criterion is chosen. When measured net radiation minus soil heat flux is positive the value is taken as a daytime value, when it is negative or equal to zero it is considered as a nighttime value. This shows good correspondence with the daily cycle of the C_n^2 signal from the LAS measurements.

3. Comparison of LAS and EC Derived Sensible and Latent Heat Fluxes

For the comparison of the LAS to the EC derived sensible heat flux a linear regression is done using a least absolute deviation technique (Birkes and Dodge, 1993). This method is chosen because of its lower sensitivity to outlying data. Regression coefficients for sensible heat flux of LAS data against EC data for all half-hour values are calculated as $H_{LAS} = a + b^* H_{EC}$. The results also include a linear regression forced through the origin (zero intercept). Additionally correlation coefficient and bias corrected root mean square error (RMSE) are calculated. For latent heat flux the same procedure is followed. For Ejura, data are divided into two periods. During the first period the prevailing wind direction is south-west, in the second period the wind direction changes more to the east. This change has major impact on energy balance closure (compare Section 4.1).

Figure 3 shows that sensible and latent fluxes from the EC system are very small during nighttime. Furthermore, during nighttime the footprint of the LAS in the upwind direction is on average four times larger compared to the EC footprint. Especially for Ejura the results are very poor (highest $R^2 = 0.1$). Therefore, the analyses are restricted to daytime values. The bad results for nighttime situations at Ejura test site might be explained by the influence of the complex terrain, resulting in a flux, which is not constant with height, and nighttime gravitational flow. Since there were no measurements at different heights, this could not be confirmed.

3.1. Sensible heat flux

Figure 3 shows a time series of 10 days for LAS and EC derived sensible heat flux for both sites. During daytime both sensors show comparable results for H. During nighttime sensible heat flux is higher for most of the nights for the LAS based measurements.

Table II shows the results of the comparison between measured sensible heat flux from EC and LAS measurements for the two sites. The linear regression for sensible heat flux gives reasonable results with a slope of 1.1 and a small intercept for Tamale. This confirms that the diurnal cycle for sensible heat flux is represented well by both systems (compare Figure 3). For sensible heat flux at the Ejura test site the results are not as good as for Tamale. The linear regression gives a lower slope and higher intercept. For both sites Figure 4 shows scatter plots for H_{LAS} versus H_{EC}. For Tamale the amount of scatter increases for higher sensible heat flux. Furthermore there is an overestimation of sensible heat flux obtained from the LAS measurements. For both sites there are a number of measurements in the low end of the measurement range, which do not correspond (compare Figure 4). This shows that for early morning hours or late afternoon hours the LAS fluxes are higher. The linear regression forced through the origin shows that for higher values of sensible heat flux the slope is closer to one (Table II).

The large amount of scatter for Ejura confirms the low correlation and high RMSE for Ejura. The lower correlation compared to Tamale is due to higher random errors, which is also demonstrated by a higher RMSE. The higher random errors might be due to the fact that the terrain at the test site in Ejura is more heterogeneous than at Tamale.

The assumption behind the comparison of the two methods is that the EC system has been installed to "see" a subsample of the LAS footprint, because it is installed in the centre of the path and at a lower height. Both sensors should "see" comparable surfaces, large enough to average out the small-scale inhomogeneities. They should give comparable results as long as the size of the EC footprint is larger than the size of the inhomogeneities. For situations where the size of the EC footprint is marginal compared to the size of the inhomogeneities, scatter is introduced. In the present study an approximate analytical footprint model (Hsieh et al.,

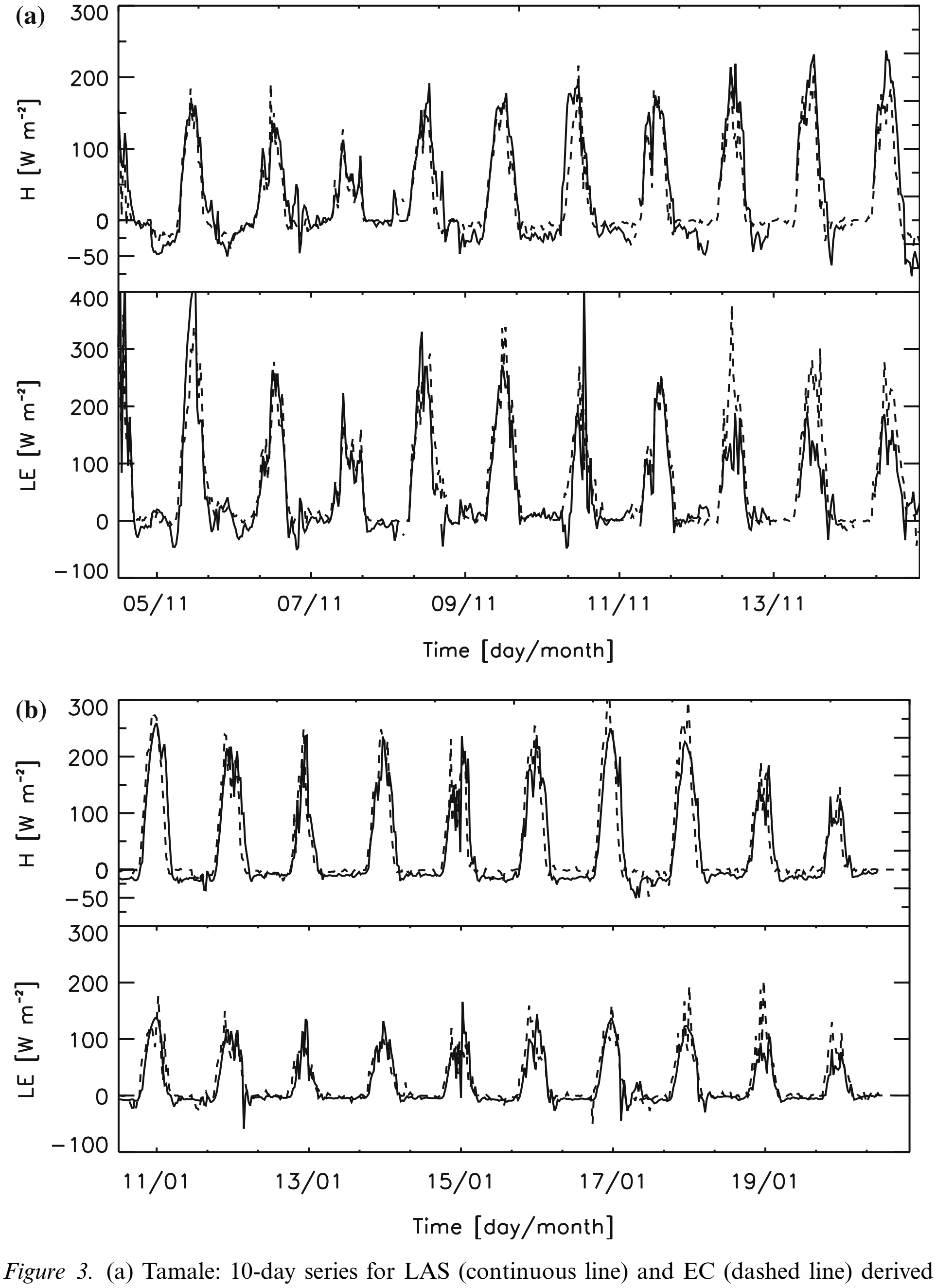

Figure 3. (a) Tamale: 10-day series for LAS (continuous line) and EC (dashed line) derived sensible and latent heat flux after the rain had stopped for more then one month. (b) Same as (a) for Ejura.

TABLE II
Comparison of sensible and latent heat flux.

	Sensible Heat Flux				Latent Heat Flux			
ID	Intercept	Slope	R^2	RMSE	Intercept	Slope	R^2	RMSE
Units	W m^{-2}			W m^{-2}	W m^{-2}			W m^{-2}
(a) For daytime from LAS and EC for the IOP in Tamala[a]								
Normal	5.3	1.10	0.86	34.0	34.0	0.69	0.67	63.8
Zero intercept	0.0	1.07	0.87	34.0	0.0	0.93	0.67	63.8
(b) From LAS and EC for the IOP in Ejura[b]								
Period until DOY 345	12.2	0.81	0.67	53.4	34.5	0.36	0.60	73.6
Zero intercept	0.0	1.08	0.67	53.4	0.0	0.8	0.61	73.6
Period from DOY 346	19.2	0.88	0.70	52.1	30.7	0.40	0.65	60.1
Zero intercept	0.0	1.01	0.71	52.1	0.0	0.86	0.68	60.1

[a]start at DOY 307 and end at DOY 349 in 2002.
[b]Ejura divided into two periods, due to the change in wind direction (start at DOY 313 in 2002 and end at DOY 28 in 2003).

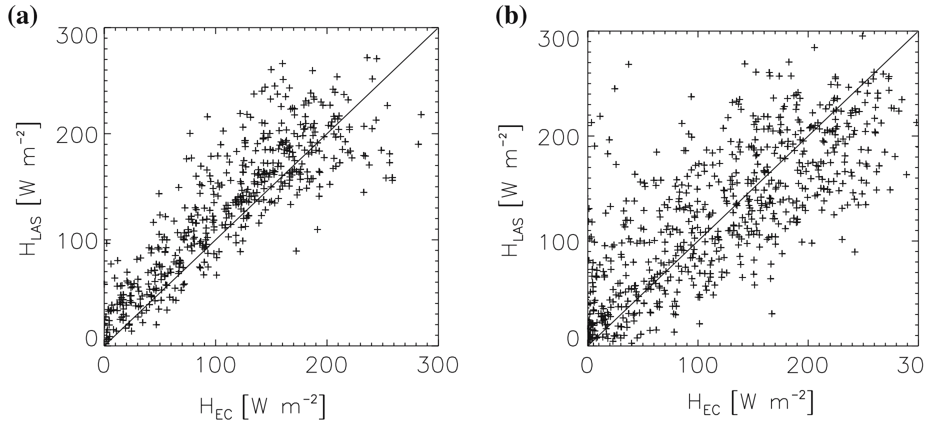

Figure 4. (a) Tamale: EC derived sensible heat flux versus LAS derived sensible heat flux. Scatter plot for the analysed period during the IOP with daytime values only. (b) Same as (a) for Ejura.

2000) is used, based on a combination of Langrangian stochastic dispersion model results and dimensional analysis. It is utilized to determine the source distance in the upwind direction, where 90% of the flux originates from. For both test sites and systems the model calculated that in 98% of the cases 90% of the flux originated within 600 m in the upwind direction for unstable cases (Figure 5). For stable situations the source area gets very large and the flux originated in only 18% of all cases from the first 10,000 m in the upwind direction, with higher values for the LAS based measurements. The percentage of observations that originate from an area with a length of at most the median of the distance between the trees equals 5% for Tamale and 11% for Ejura. This percentage of the data could scatter due to incomparable footprints. From the footprint analysis and Figure 4 it is concluded that in Tamale the surface properties in the footprint of both systems are comparable more often than in Ejura. From Figure 5 it is also concluded that the EC system sees a rather small subsample of the LAS path, since the diameter of the plotting-circle is not even the path length of the LAS. For Ejura there are also differences in surface properties on a larger scale. This might explain even more scatter.

As a first approximation the source area of the LAS can be calculated by multiplying the footprint in the upwind direction with the part of the LAS path that covers 90% of the contribution to C_n^2, based on the weighting function of the LAS. For both sites the size of the source area of a LAS is larger when the wind direction is not parallel to the path (compare also Meijninger et al., 2002).

3.2. Latent heat flux

Figure 3 shows that for most of the days the LE_{LAS} and LE_{EC} correspond well during the diurnal cycle. During the night LE is close to zero for both systems. For the comparisons of the LAS derived latent heat flux and EC data in Tamale the correlation is lower compared to sensible heat flux. The linear regression shows an underestimation of the latent heat flux calculated from the residual of the energy balance (Equation 4). For Ejura the results are not as good as for Tamale. Since for Ejura no measurements were available to calculate the correct soil heat flux at the soil surface, there is an error in the calculation for latent heat flux from LAS data. However, due to the more dense vegetation cover, this effect should be smaller than at Tamale. Linear regression forced through the origin gives better results, which shows that the main deviations in latent heat flux occur during early morning and late afternoon hours. The correlation coefficient is not as good as for sensible heat flux and the RMSE is large for both sites given a maximum flux of about 250 W m^{-2}.

4. Evaluation of the Energy Balance Closure

For the energy balance closure it is important to remember the reasons for nonclosure mentioned in the introduction. Sampling errors are closely related to the different footprints of the components of the energy balance.

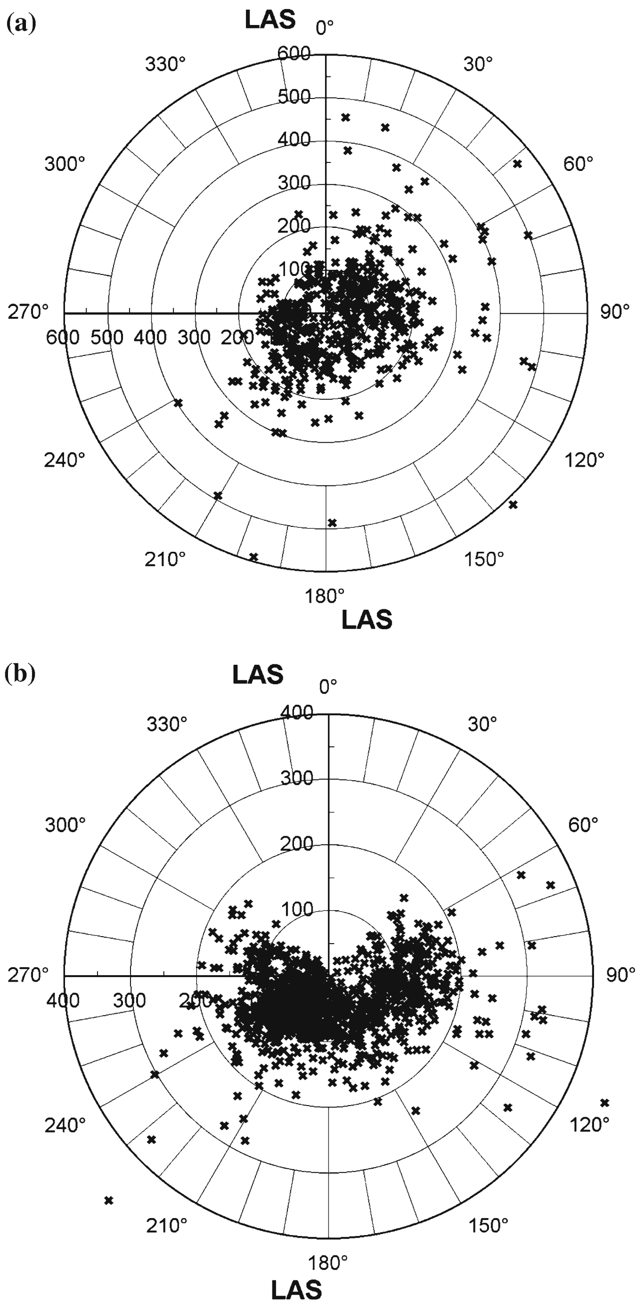

Figure 5. (a) Source distance in m of sensible heat flux depending on wind direction during unstable situations. Polar plot for the analysed period during the IOP in Tamale. (b) Same as (a) for Ejura.

Net radiation and soil heat flux will never have the same footprint as sensible and latent heat flux. For soil heat flux the footprint is always much smaller than for all other components of the energy balance. For net radiation, which is the largest component of the energy balance, other studies have found little spatial variability over different kinds of terrain (Stannard et al., 1994; Twine et al., 2000) and errors that are up to a maximum of 6% (Moncrieff, 1996) are often assumed. One crucial point for net radiation is that there exists no widely accepted or standard method for measuring and that errors in factory calibration for different sensors can be larger then the accuracy (Halldin and Lindroth, 1992). Cobos and Baker (2003) tested the net radiometer, which is used in this study (NR Lite, Kipp & Zonen) and found good agreement with the summation of the four independently measured components of net radiation under most field conditions. However, precipitation and condensation affect the performance, but the influence is negligible for Tamale and small for Ejura. The variability in net radiation and soil heat flux also shows that independent measured fluxes are needed for comparison (at least for IOPs) when latent heat flux is calculated as a residual from the energy balance.

For the evaluation of the energy balance closure, different methods are used. The first method is to calculate the cumulative sum of the available energy ($R_n - G$) and the dependent fluxes ($\mathrm{LE} + H$) over the analysed periods and calculate the Energy Balance Ratio (EBR) (Gu et al., 1999).

$$\mathrm{EBR} = \frac{\sum(\mathrm{LE} + H)}{\sum(R_n - G)}. \tag{5}$$

This is a first means to illustrate an overall evaluation for the IOP. The advantage of this method is that it neglects possible random errors in flux estimation. The second method is the derivation of linear regression coefficients for available energy ($R_n - G$) and the dependent fluxes ($\mathrm{LE} + H$). The linear regression is done again using the least absolute deviation technique. This is even more important here since random errors for measured net radiation and soil heat flux cannot be specified properly. Regression coefficients are calculated for ($\mathrm{LE} + H$) against ($R_n - G$) using the following relationship $(\mathrm{LE} + H) = a + b^*(R_n - G)$. Energy balance closure is evaluated with sensible heat flux from the LAS and from EC data, also to gain more confidence in the gathered data. This is especially important for further applications during periods where there are no EC data available. For both cases LE is obtained from the EC data.

Since the magnitude of the imbalance of the energy balance closure often shows a close relationship to the diurnal cycle the residual in the relative energy imbalance (REI) is calculated as well to get more insights about the instantaneous errors. In contrast to the EBR, where the cumulative sum of the available energy and the dependent fluxes over the analysed periods is calculated, the REI is calculated for each half-hour interval. It is defined as follows:

$$\mathrm{REI} = \frac{R_\mathrm{n} - G - \mathrm{LE} - H}{R_\mathrm{n} - G}. \tag{6}$$

After calculating REI the data are grouped into three classes. The first class only contains data where the absolute $\mathrm{REI} \leq 0.10$ This corresponds to an instantaneous error smaller then 10% during each individual interval and therewith an acceptable closure of the energy balance. The second group contains only data where $\mathrm{REI} > 0.10$ (positive bias) and the third group contains data where deviations in $\mathrm{REI} < -0.1$ (negative bias).

4.1. Surfaces fluxes on a seasonal basis

Figure 6 shows daily averages of surface fluxes LE and H as well as G and net radiation for the IOP at both sites. Surface flux data are mainly taken from the EC system. During small gaps due to data logger failure LAS data are used. There is a clear decline in net radiation towards the end of the period mainly due to the decline in incoming solar radiation in combination with changing surface conditions. For soil heat flux there is a small rise from the beginning to the end. For Tamale sensible heat flux shows an increase from the beginning to the end and a clear decline in latent heat flux. For Ejura sensible heat flux remains nearly at one level from the beginning to the end. There is a small decline in latent heat flux during November, but for the rest of the IOP it stays on the same level. It is also evident that latent heat flux is not negligible until the end of the IOPs. The last rain event appeared during DOY 343 in Ejura. In Tamale that was during DOY 287. This demonstrates that for large parts of the dry season the plants are able to evaporate. One reason for the ongoing evapotranspiration is the deep rooting system of the trees. The trees are still green and transpiration continues.

For Ejura Figure 6b shows that there exists a systematic error in the closure of the energy balance until a certain time of the year. Those findings are in contrast to the results of Tamale. The error in the closure of the energy balance corresponds well with a change in wind direction, thus coinciding with a sudden increase in VPD. The error in the beginning of the IOP at Ejura test site shows that there is a clear advective influence on the closure of the energy balance. During the period until DOY 345 the prevailing wind direction is south-west, resulting in winds from a steep slope (> 12%). As soon as the wind direction changes more to the east (sector with mild topography) the energy balance closes better. This effect on the closure of the energy balance is already observed by Lee and Hu (2002). At the end of the IOP the wind direction changes again more to

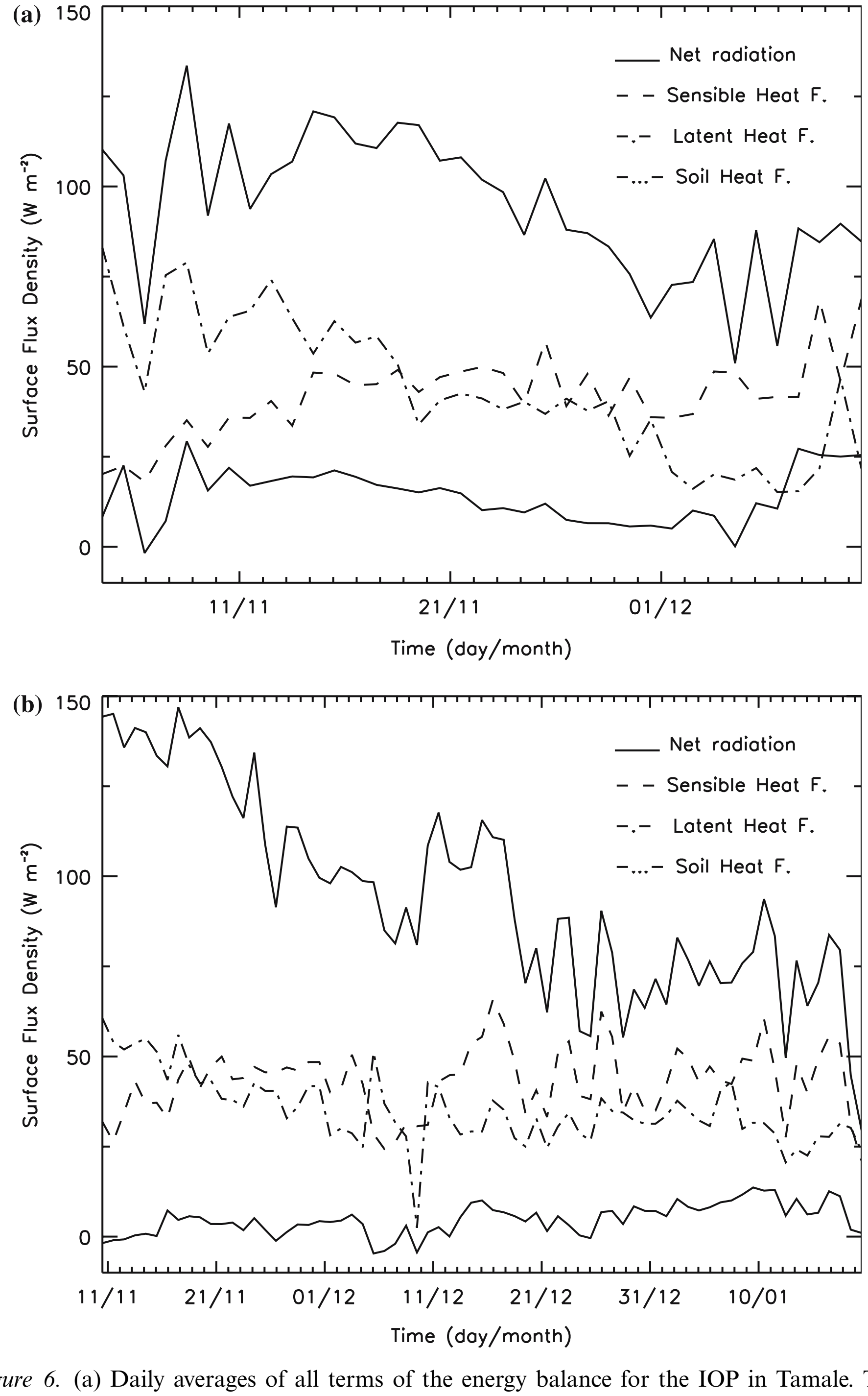

Figure 6. (a) Daily averages of all terms of the energy balance for the IOP in Tamale. Turbulent flux data are mainly taken from the EC measurements. (b) Same as (a) for Ejura. Note the difference in time period.

TABLE III
Evaluation of energy balance closure for day and nighttime values with measurements from LAS and EC.

ID Units	Intercept Wm^{-2}	Slope	R^2	EBR
(a) Tamle (for the IOP)				
With H EC day	6.8	0.98	0.87	0.97
With H LAS day	−4.7	0.99	0.87	1.00
With H EC night	−14.9	0.42	0.32	0.21
With H LAS night	−12.5	0.31	0.38	0.99
(b) Ejura (for the whole period)				
With H EC day	58.0	0.87	0.82	0.80
With H LAS day	33.7	0.95	0.77	0.85
With H EC night	−16.2	0.14	0.07	0.03
With H LAS night	−15.7	0.16	0.10	1.10

the south-west, but this time not resulting in worse closure of the energy balance. A possible reason could be the better turbulent mixing by the end of the IOP.

Since the results for the two sites differ in several aspects, further evaluation is done for the two sites separately.

4.2. Tamale

The results show a nearly perfect energy balance closure with both methods during the day, considering the slope of the linear regression as well as the EBR (Table IIIa), which suggests that the daily cycle is represented realistically and also on the long term there are only small errors. For nighttime situations the results show a large difference between the LAS and the EC based measurements. The slope is larger for the EC based measurements. This has to be seen in context of the low R^2, which is associated with larger random errors. The EBR, which should not be affected by random errors, shows better results for the LAS based measurements as well.

The relative energy imbalance (REI) was analysed in this context to get more insights in the instantaneous closure of the energy balance in contrast to the long-term closure expressed by the EBR. Therefore, the REI is calculated for every daytime and nighttime value. For daytime values the median of REI with sensible heat flux from the EC system is 0.05 and for energy balance closure based on sensible heat flux from LAS it is found to be −0.05. The percentage of acceptable REI with $|\text{REI}| \leq 0.10$ for the energy balance with H from EC is 31.6% and for the LAS based H it is 29.6%. The positively biased class for the EC based system comprises 38% of the observations and is larger than the negatively biased class with 29%. For the LAS based system it is the other way around (negative bias = 27.1%; positive bias = 43.2%). To obtain more insights into the instantaneous closure, the daytime values are divided into morning and afternoon hours. Both systems give the largest deviation in the afternoon, where turbulence normally reaches its highest values. The LAS overestimates the sum of the turbulent fluxes by 27.2% and the EC systems underestimates by 23%. This is different compared to other studies (e.g. Wilson et al., 2002), which show larger errors in the morning due to storage terms. For nighttime values the EC based data show a systematic error since the sum of dependent fluxes is too low in 93% of all cases. For the LAS based system the percentage of too high and too low REI is nearly equal, which means there is no systematic error. Further analyses show that more then 60% of the measurements show a $|\text{REI}| \leq 0.50$.

4.3. Ejura

The energy balance closure is evaluated in the same way as in Tamale. As a first step the energy balance closure is evaluated for the whole period with sensible heat flux from the LAS and from EC data. Regression coefficients are calculated for $\text{LE} + H$ against $R_n - G$ (Table IIIb). The EBR during daytime and nighttime is higher for the LAS measurements. Linear regression gives better results for daytime situations for LAS measurements. This is partly due to the fact that during the first period the LAS gives a higher sensible heat flux compared to the EC system. For nighttime values the results are similar for both systems concerning the linear regression, but are on a low level.

The instantaneous closure expressed with REI during daytime shows an underestimation for both systems. The median of the REI is found with sensible heat flux from the EC system to be 0.20 and for energy balance based on sensible heat flux from LAS it was found to be 0.17. The percentage of acceptable REI with $|\text{REI}| \leq 0.10$ for the energy balance with H from EC is 23.5% and for the LAS based H it is 22.3%. The positively biased class for the LAS and the EC based system is higher (EC = 58.5%; LAS = 58.8%) than the negatively biased class (EC = 18%; LAS = 18.8%). This becomes even clearer when the dataset is divided again into morning and afternoon classes. Both systems show an underestimation of sensible and latent heat flux during the afternoon hours up to 45%. This might partly be explained by the non-adjusted soil heat flux. It imposes an error in phase, which leads to too high values during the afternoon hours.

For nighttime the same systematic error is observed for the EC based system as in Tamale, whereas the error is nearly equally distributed for the LAS based system. For the LAS based system more then 70% of the measurements show $|REI| \leq 0.50$.

In a second step data were divided into the already mentioned two periods (see Section 3). The EBR is higher for both periods, when sensible heat flux is taken from the LAS (0.71 and 0.95 compared to 0.64 and 0.90 for the EC based system). The same trend is seen in the linear regression. The third step is to evaluate if the closure of the energy balance can be improved by calculating the Bowen Ratio (β) from the EC measurements, assuming that the Bowen Ratio is estimated correctly by the EC system (Twine et al., 2000). With the help of the calculated Bowen Ratio a corrected latent heat flux is estimated in the following way:

$$\mathrm{LE}_{\mathrm{corr}} = \frac{H_{\mathrm{LAS}}}{\beta}. \tag{7}$$

For the first period the EBR now equals 0.76 compared to 0.71 with H_{LAS} and $\mathrm{LE}_{\mathrm{EC}}$ and 0.64 for H_{EC} and $\mathrm{LE}_{\mathrm{EC}}$. For the whole period the EBR now is 1.0, which is an improvement compared to the LAS based EBR of 0.85. This demonstrates that a simple way of adjusting surface fluxes by using the Bowen Ratio helps in improving the energy balance closure. This might be useful in further model studies.

5. Evaluation of Surface Conductance

The surface conductance (g_{s}) is calculated with the rearranged Penman–Monteith equation (e.g., Monteith and Unsworth, 1990) following the notation by Harris et al. (2003):

$$g_{\mathrm{s}} = g_{\mathrm{a}} \left[\frac{\Delta (R_{\mathrm{n}} - G) + \rho c_{\mathrm{p}} VPD g_{\mathrm{a}}}{\gamma LE} - \frac{\Delta}{\gamma} - 1.0 \right]^{-1}. \tag{8}$$

Here Δ is the slope of saturated vapour pressure with temperature ($\mathrm{Pa\,K^{-1}}$), ρ is air density ($\mathrm{kg\,m^{-3}}$), c_{p} is specific heat of air at constant pressure ($\mathrm{J\,kg^{-1}\,K^{-1}}$), γ is the psychrometric constant ($\mathrm{Pa\,K^{-1}}$) and g_{a} is the aerodynamic conductance for water vapour ($\mathrm{m\,s^{-1}}$). With the measurements of the different components of the energy balance g_s can be calculated from Equation (8) and can be considered as the surface conductance for the water vapour transfer between the heterogeneous surface and the atmosphere. For the calculation of the aerodynamic conductance the method of Verma (1989) with stability corrections by Paulson (1970) is used. The roughness length for momentum was estimated using the approach of Martano (2000) and roughness length for heat was estimated by applying a fixed ratio of roughness length for momentum and heat of 100, which was estimated for savannah conditions by Huntingford et al. (1995). A more detailed description of the approach used can be found in Harris et al. (2003). Under conditions of low available energy the computation of g_s can give non-realistic conductances. Therefore, the calculation of g_s is restricted to daytime situations between 0900 and 1700. The surface conductance is mainly controlled by incoming solar radiation (R_g), VPD, temperature and soil moisture. Since evapotranspiration is mainly dominated by transpiration for the two sites and periods, the driving forces should mainly reflect stomatal functions.

There are a number of models utilizing the different factors named above for the calculation of surface conductance. In our study a Jarvis-type model is used given by the following equation:

$$g_s = \mathrm{LAI} \cdot g_{\max} \cdot \prod_i f_i(X_i). \tag{9}$$

The functions, f_i can have a range between 0 and 1. Following Dolman (1993) the different f_i are given by

$$f_1(D) = e^{-\mathrm{VPD}/a_1}, \tag{10}$$

$$f_2(T) = \left(\frac{T - T_L}{a_2 - T_L}\right) - \left(\frac{T_U - T}{T_U - a_2}\right)^{\tau} \quad \text{with} \quad \tau = \frac{T_u - a_2}{a_2 - T_L} \tag{11}$$

$$f_3(R_g) = \frac{R_g}{a_3 + R_g}\left(1 + \frac{a_3}{R_{g\max}}\right), \tag{12}$$

$$f_4(\Theta) = \begin{cases} 1 & \Theta < a_4 \\ \frac{a_5-\Theta}{a_5-a_4} & a_4 \le \Theta < a_5, \\ 0 & \Theta \ge a_4 \end{cases} \tag{13}$$

where T_U(°C) and T_L(°C) mark the upper and lower temperature limits where transpiration stops. T_U and T_L are set to 45 and 5°C and $R_{g\max}$ equals 1000 W m^{-2}.

Huntingford et al. (1995) optimised the different parameters $a_1, \ldots, a_5$ for savannah conditions during the wet season. We adopt those values and also retain the function f_2 in contrast to Huntingford et al. (1995). We use the findings of Harris et al. (2003) for estimating an expression for a_2. Table IV shows all values used for both test sites with the error ranges of parameters $a_1, \ldots, a_5$. From Table IV it can already be seen that some of the parameters show a large uncertainty. For $g_{\max}$ values are used from the

TABLE IV

Parameters from optimisations (Huntingford et al., 1995) of a Jarvis model of surface conductance for Savannah including maximum canopy conductance (g_{max}), leaf area index (LAI), functional dependence on solar radiation (a_1), air temperature (a_2), vapour pressure deficit (a_3), soil moisture (a_4; a_5).

ID Units	LAI $m^2 m^{-2}$	g_{max} $mm\,s^{-1}$	a_1 $W\,m^{-2}$	a_2 °C	a_3 $g\,kg^{-1}$	a_4 mm	a_5 mm
Tamale	1	10.0	36.5 ± 10.0	25.0 ± 4.5	36.7 ± 50.0	47.6 ± 50.0	153.0 ± 20.0
Ejura	4	4.16	36.5 ± 10.0	25.0 ± 4.5	36.7 ± 50.0	47.6 ± 50.0	153.0 ± 20.0

LAI and g_{max} are taken from the regionally dependent USGS database (http://edcdaac.usgs.gov/glcc/af_int.asp).

USGS NOAA global dataset (http://edcdaac.usgs.gov/glcc/af_int.asp), which is widely used by modellers.

The Jarvis-type approach is fairly "well-established" and the functions f_i have been optimised for a lot of regions. In this study our focus is not on optimising but on testing the response of the surface conductance to the functions f_i during the time of transition, since it is very difficult to develop a single solution under the influence of multiple feedback processes that mask the interactions.

For both test sites the measured and modelled canopy conductances show a large variability during the examined periods (Figure 7). For Ejura the surface conductance obtained by the rearranged Penman–Monteith equation shows a large decrease during the first period of the IOP. From the part of the IOP when the energy balance closes better and the VPD rises it remains low. This is important since the closure of the energy balance during the first period was not as good as for the second period, which means that for the further analyses only the second period was considered.

The important factors to model the surface conductance correctly are the different functions that control the response on different time scales. Soil moisture dependence and VPD dependence are needed to produce reasonable results for the seasonal cycle. Both variables change significantly at both test sites (Figure 7), whereas temperature and incoming solar radiation do not change significantly. The surface conductance decreases approximately linear during the day (Figure 8) (at least from 0900 to 1700 pm) but during the IOP the slope of this decrease gets less steep for Tamale. For Ejura the starting and end points stay nearly constant during the IOP. The relatively stable surface conductance during the second period in Ejura also shows that the plants are able to transpire during the drying up due to the deep rooting systems.

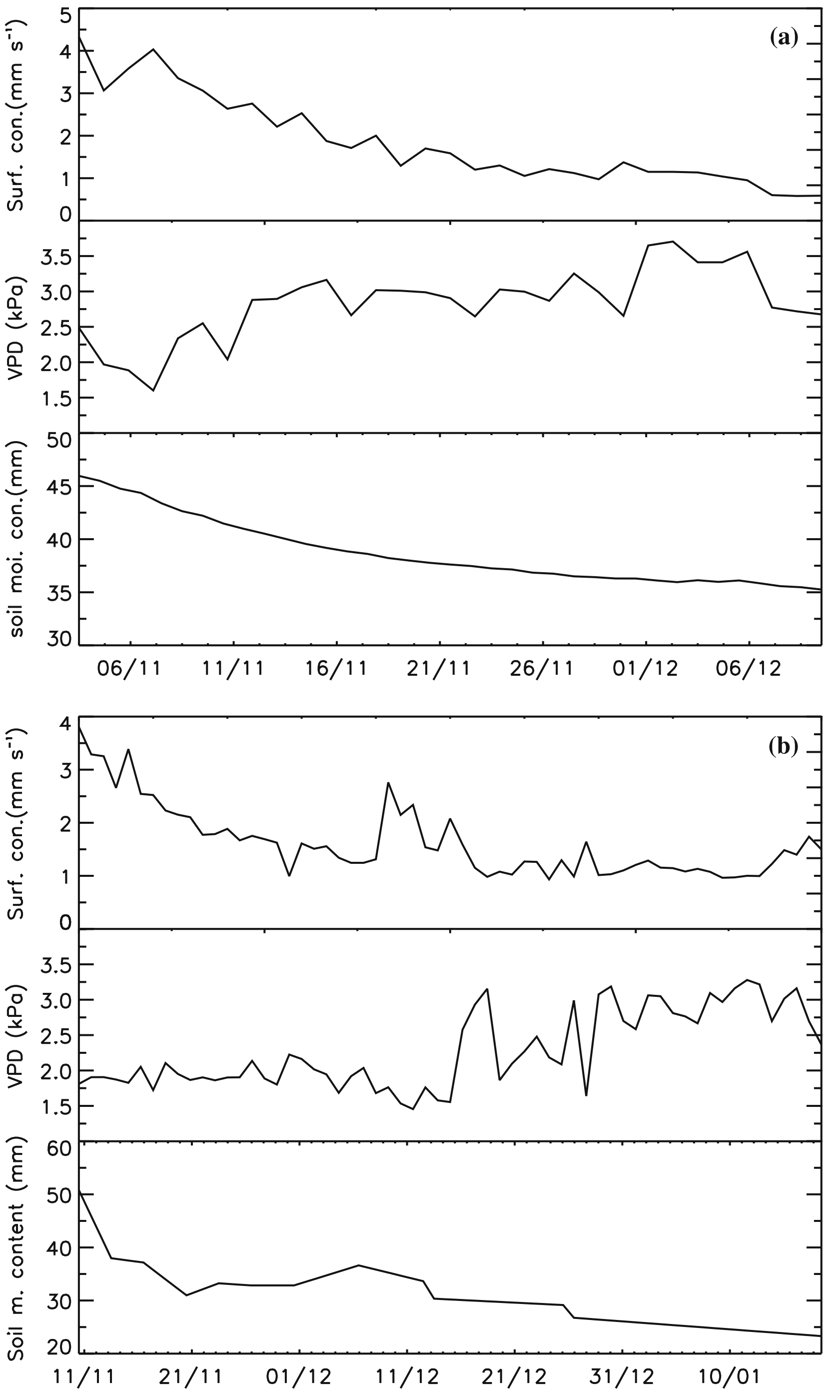

Figure 7. (a) Daily median of surface conductance, daily mean of VPD and daily mean of soil moisture content for the IOP in Tamale. (b) Same as (a) for Ejura. Note the difference in time period.

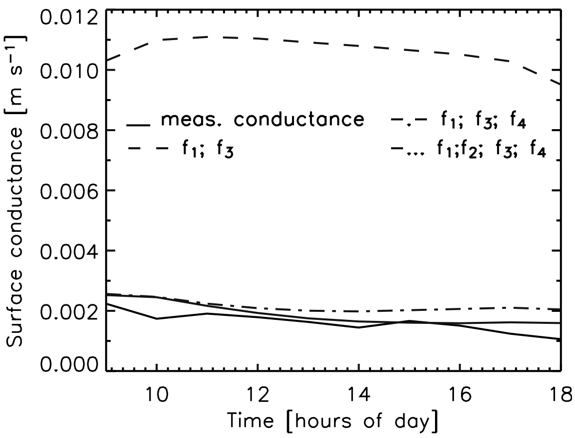

Figure 8. Illustration of the mean diurnal course of measured and modelled surface conductance for a 5-day period in Tamale starting at the 14th November 2002. For the modeled g_s, the results with different combinations of function f_i are shown.

TABLE V

Average μ and the class of μ with maximum deviations of $|0.2|$ for both test sites taking the four different response functions for the Jarvis-type model into account.

Jarvis function	Average μ		% with $\|\mu\| \leq 0.2$	
	Tamale	Ejura	Tamale	Ejura
$f_1 f_3$	0.16	0.10	< 5%	< 5%
$f_1 f_2 f_3$	0.20	0.16	< 5%	< 5%
$f_1 f_3 f_4$	0.75	0.82	30%	35%
$f_1 f_2 f_3 f_4$	0.93	0.96	40%	41%

To analyse the errors in modelled g_s half-hourly values of the dimensionless ratio μ:

$$\mu = \frac{g_s}{g_{s\,mod}}, \tag{14}$$

were calculated for the IOPs during the hours from 0900 to 1700. Theoretically μ should always equal 1. The average μ and the percentage of μ with maximum deviations of $|0.2|$ are shown in Table V.

When soil moisture (f_4) and temperature dependence (f_2) are not included, the conductance is highly overestimated during the whole day (compare also Figure 8). Including only temperature dependence gives a more realistic decrease for g_s during the day, but the total level is still too high. As soon as soil moisture dependence is included the results are improved and even get better when temperature dependence is included again. The higher percentage of $|\mu| \leq 0.2$ shows that including temperature dependence helps in modelling surface conductance correctly. The better results when temperature dependence is included could not be achieved by only varying the VPD response function (f_1) by varying a_1, since values for a_1 would be needed, that would have been out of the error ranges to achieve similar results.

When those findings are compared to those of Huntingford et al. (1995) it is seen that temperature has a more pronounced diurnal cycle during the time of transition compared to the measurements of Huntingford et al. (1995), which were taken during the wet season.

6. Conclusions

Three important conclusions can be drawn from this study. First, the GLOWA-Volta project has generated a land surface dataset in a semi-arid region in West Africa. The data show a good quality and consistency, suitable for further application in the future.

The second conclusion is that the measured energy balance closes well for Tamale test site. The closure for the Ejura test site improves during the time of transition. The relative energy imbalance (REI) shows the largest errors in the afternoon, which makes it different from most of the other measurements, which show the largest errors in the morning due to storage terms.

The third conclusion is that for the region during the process of drying up a Jarvis-type model works better when temperature dependence is taken into account. The influence of temperature is also important with the background of simulations of future climate, in which many global climate models predict higher near surface temperatures for West Africa.

For modelling evapotranspiration correctly proper soil moisture estimation is crucial, which suggests the need to test more sophisticated land surface models in the future, which take soil physical properties, root distribution and deeper soil moisture content into account.

Acknowledgements

This research was sponsored by the Federal Ministry of Education and Research, Germany. The authors would like to thank Raymond Kasei, Ronald Groen and Gabriel Akotia for assistance in the field and two anonymous reviewers for their constructive comments on the first version of this study.

References

Agyare, W.: 2004, 'Soil Characterization and Modeling of Spatial Distribution of Saturated Hydraulic Conductivity at Two Sites in the Volta Basin of Ghana', *Ecology Develop. Series* Vol. 17, 194 pp.

Baldocchi, D., Falge, E., Gu, L., Olson, R., Hollinger, D., Running, S., Anthoni, P., Bernhofer, Ch., Davis, K., Evans, R., Fuentes, J., Goldstein, A., Katul, G., Law, B., Lee, X., Malhi, Y., Meyers, T., Munger, W., Oechel, W., Paw, K. T., Pilegaard, K., Schmid, H. P., Valentini, R., Verma, S., Vesala, T., Wilson, K., and Wofsy, S.: 2001, 'FLUXNET: A New Tool to Study the Temporal and Spatial Variability of Ecosystem-Scale Carbon Dioxide, Water Vapor, and Energy Flux Densities', *Bull. Amer. Meteorol. Soc.* **82**, 2415–2434.

Baldocchi, D., Xu, L., and Kiang, N.: 2004, 'How Plant Functional-Type, Weather, Seasonal Drought, and Soil Physical Properties Alter Water and Energy Fluxes of an Oak-Grass Savanna and an Annual Grassland', *Agric. For. Meteorol.* **65**, 21–45.

Birkes, D. and Dodge, Y.: 1993, *Alternative Methods of Regression*, John Wiley and Sons, Inc., New York, 228 pp.

Bolle, H.-J., Andre, J. C., and Arrue, J. L.: 1993, 'EFEDA: European Field Experiment in a Desertification-Threatened Area', *Ann. Geophys.* **11**, 173–189.

Burpee, R. W.: 1972, 'The Origin and Structure of Easterly Waves in the Lower Troposphere of North Africa', *J. Atmos. Sci.* **29**, 77–90.

Cobos, D. R. and Baker, J. M.: 2003, 'Evaluation and Modification of a Domeless Net Radiometer', *Agron. J.* **95**, 177–183.

De Bruin, H. A. R., Kohsiek, W., and van den Hurk, B. J. J. M.: 1993, 'A Verification of Some Methods to Determine the Fluxes of Momentum, Sensible Heat, and Water Vapor Using Standard Deviation and Structure Parameter of Scalar Meteorological Quantities', *Boundary-Layer Meteorol.* **63**, 231–257.

De Bruin, H. A. R., van den Hurk B. J. J. M., and Kohsiek, W.: 1995, 'The Scintillation Method Tested Over a Dry Vineyard Area', *Boundary-Layer Meteorol.* **93**, 453–468.

Dolman, A. J.: 1993, 'A Multiple-Source Land Surface Energy Balance Model for Use in General Circulation Models', *Agric. For. Meteorol.* **65**, 21–45.

FAO Report: 1984, Agroclimatological Data for Africa. No. 22, Vol.1: Countries North of the Equator. Food and Agriculture Organization (FAO) of the United Nations, Rome.

Foken, Th. and Wichura, B.: 1996, 'Tools for Quality Assessment of Surface-Based Flux Measurements', *Agric. For. Meteorol.* **78**, 83–105.

Friesen, J.: 2002, *Spatio-temporal Patterns of Rainfall in Northern Ghana*, Diploma thesis, University of Bonn, 81 pp.

Goutorbe, J.-P., Lebel, T., and Tinga, A.: 1994, 'HAPEX-Sahel: A Large-Scale Study of Land-Atmosphere Interactions in the Semiarid Tropics', *Ann. Geophys.* **12**, 53–64.

Gu, J., Smith, E. A., and Merritt, J. D.: 1999, 'Testing Energy Balance Closure with Goes Retrieved Net Radiation and in Situ Measured Eddy Correlation Fluxes in BOREAS', *J. Geophys. Res.,* **104**, 27–81.

Halldin, S. and Lindroth, A.: 1992, 'Errors in Net Radiometry: Comparison and Evaluation of Six Radiometer Designs', *J. Atmos. Oceanic Technol.* **9**, 762–783.

Harris, P. P., Huntingford, C., Cox, P. M., Gash, J. H. C., and Malhi, Y.: 2003, 'Effect of Soil Moisture on Canopy Conductance of Amazonian Rainforest', *Agric. For. Meteorol.* **122**, 215–227.

Hartogensis, O. K., Watts, C. J., Rodriguez, J.-C., and De Bruin, H. A. R.: 2003, 'Derivation of a Effective Height for Scintillometers: La Poza Experiment in Northwest Mexico', *J. Hydrometeorol.* 4, 915–928.

Heusinkveld, B., Jacobs, A. F. G., Holtslag, A. A. M., and Berkowicz, S. M.: 2004, 'Surface Energy Balance Closure in an Arid Region: Role of Soil Heat Flux', *Agric. For. Meteorol.* **122**, 21–37.

Hólm, E., Andersson, E., Beljaars, A., Lopez, P., Mahfouf, J. F., Simmons, A., and Thépaut, J. N.: 2002, *Assimilation and Modeling of the Hydrological Cycle: ECMWF's Status and Plans*.

Hsieh, C. I., Katul, G. G., and Chi, T. W.: 2000, 'An Approximate Analytical Model for Footprint Estimation of Scalar Fluxes in Thermally Stratified Atmospheric Flows', *Adv. Water Res.* **23**, 765–772.

Huntingford, C., Allen, S. J., and Harding, R. J.: 1995, 'An Inter-Comparison of Single and Dual-Source Vegetation-Atmosphere Transfer Models Applied to Transpiration from Sahelian Savannah', *Boundary-Layer Meteorol.* **74**, 397–418.

Jarvis, P.: 1976, 'The Interpretation of the Variations in Leafwater Potentials and Stomatal Conductances Found in Canopies in the Field', *Philos. Trans. Rof. Soc. London Ser. B* **273**, 593–610.

Kasei, C. N.: 1988, 'The Physical Environment of Semiarid Ghana', in: P. W. Unger , T. V. Sneed, W. R. Jordan, and R. Jensen, (eds.), *Challenges in Dryland Agriculture – A Global Perspective.* Texas Agricultural Experiment Station, Amarillo/Bushland, pp. 350–354.

Lamaud, E., Ogée, J., Brunet, Y., and Berbigier, P.: 2001, 'Validation of Eddy Flux Measurements Above the Understorey of a Pine Forest', *Agric. For. Meteorol.* **106**, 173–186.

Lee, X. and Hu, X.: 2002, 'Forest-Air Fluxes of Carbon, Water and Energy over Non-Flat Terrain', *Boundary-Layer Meteorol.* **103**, 277–301.

Mahrt, L.: 1998, 'Flux Sampling Errors for Aircrafts and Towers', *J. Atmos. Oceanic Tech.* **15**, 416–429.

Martano, P.: 2000, 'Estimation of Surface Roughness Length and Displacement Height from Single-Level Sonic Anemometer Data', *J. Appl. Meteorol.* **39**, 708–715.

Meijninger, W. M. L., Green, A. E., Hartogensis, O. K., Kohsiek, W., Hoedjes, J. C. B., Zurbier, R. M., and De Bruin, H. A. R.: 2002, 'Determination of Area-Averaged Water Vapor Fluxes with Large Aperture and Radio Wave Scintillometers over a Heterogeneous Surface Flevoland-Field-Experiment', *Boundary-Layer Meteorol.* **105**, 63–83.

Moene, A. F.: 2003, 'Effects of Water Vapour on the Structure Parameter of the Refractive Index for Near-Infrared Radiation', *Boundary-Layer Meteorol.* **107**, 635–653.

Moncrieff, J. B.: 1996, 'The Propagation of Errors in Long-Term Measurements of Land Atmosphere Fluxes of Carbon and Water', *Global Change Biol.* **2**, 231–240.

Monteith, J.: 1981, 'Evaporation and Surface Temperature', *Quart. J. Roy. Meteorol. Soc.* **107**, 1–27.

Monteith, J. and Unsworth, M. H.: 1990, *Principal of Environmental Physics*, (2nd ed.), Arnold, London, 291 pp.

Moore, C.: 1986, 'Frequency Response Corrections for Eddy Correlation Systems', *Boundary-Layer Meteorol.* **37**, 17–35.

Obukhov, A. M.: 1960, 'Structure of Temperature and Velocity Fields Under Conditions of Free Convection', *Works Inst. Theor. Geophys. Acad. Sci. USSR* **1**, 95–115.

Paulson, C.: 1970, 'The Mathematical Representation of Wind Speed and Temperature Profiles in the Unstable Atmospheric Surface Layer', *J. Appl. Meteorol.* **9**, 857–861.

Schaap, M. G., Leij, F. J., and van Genuchten, M. Th.: 1998, 'Neural Network Analysis for Hierarchical Prediction of Soil Water Retention and Saturated Hydraulic Conductivity', *Soil Sci. Soc. Am.* **62**, 847–855.

Schotanus, P., Nieuwstadt, F., and De Bruin, H. A. R.: 1983, 'Temperature Measurement with a Sonic Anemometer and Its Application to Heat and Moisture Fluxes', *Boundary-Layer Meteorol.* **26**, 81–93.

Solbrig, O. T., Medina, E., and Silva, J. F. (eds.): 1996, 'Determinants of Tropical Savannas', in *Biodiversity and Savanna Ecosystem Processes – A Global Perspective, Ecological Studies* Vol. 121. Springer, Berlin.

Stannard, D. I., Branford, J. H., Kustas, W. P., Nichols, W.D., Amer, S. A., Schmugge, T. J., and Weltz, M. A.: 1994, 'Interpretation of Surface Flux Measurements in Heterogeneous Terrain During the Monsoon'90 Experiment', *Water Resour. Res.* **30**, 1227–1239.

Stull, R. B.: 1988, *An Introduction to Boundary Layer Meteorology*, Kluwer Acad., Norwell, Mass, 666 pp.

Twine, T. E., Kustas, W. P., Norman, J. M., Cook, D. R., Houser, P. R., Meyers, T. P., Prueger, J. H., Starks, P. J. and Wesely, M. L.: 2000, 'Correcting Eddy-Covariance Flux Underestimates over a Grassland', *Agric. For. Meteorol.* **103**, 279–300.

Van de Giesen, N., Kunstmann, H., Jung, G., Liebe, J., Andreini, M., and Vlek, P. L. G.: 2001, 'The GLOWA Volta Project: Integrated Assessment of Feedback Mechanisms between Climate, Landuse, and Hydrology', *Adv. Glob. Change Res.* **10,** 151–170.

Van Dijk, A., Kohsiek, W., and De Bruin, H. A. R.: 2003, 'Oxygen Sensitivity of Krypton and Lyman-alpha Hygrometers', *J. Atmos. Oceanic Tech.* **20**, 143–151.

Verhoef, A., Allen, S. J., De Bruin, H. A. R., Jacobs, C. M. J., and Heusinkveld, B. G.: 1996a, 'Fluxes of Carbon Dioxide and Water Vapour from a Sahelian Savanna', *Agric. For. Meteorol.* **80**, 231–248.

Verhoef, A., van den Hurk, B. J. J. M., Jacobs, A. F. G., and Heusinkveld, B. G.: 1996b, 'Thermal Soil Properties for Vineyard (EFEDA-I) and Savanna (HAPEX-Sahel) Sites', *Agric. For. Meteorol.* **78**, 1–18.

Verma, S.: 1989, 'Aerodynamic Resistances to Transfers of Heat, Mass and Momentum in Estimation of Areal Evaporation', *IAHS Publ.* 177 pp.

Viterbo, P. and Beljaars, C.: 1995, 'An Improved Land Surface Parametrization Scheme in the ECMWF Model and its Validation', *J. Climate*. **8**, 2716–2748.

Wallace, J. S., Allen, S. J., Culf, A. D., Dolman, A. J., Gash, J. H. C., Holwill, C. J., Lloyd, C. R., Stewart, J. B., Wright, I. R., Sivakumar, M. V. K., and Renard, C.: 1992, *SEB-EX: The Sahelian Energy Balance Experiment*, ODA Report no. 92/9. IH, Wallingford, UK. 51 pp.

Webb, E., Pearman, G., and Leuning, R.: 1980, 'Correction of Flux Measurements for Density Effects Due to Heat and Water vapour Transfer', *Quart J. Roy. Meteorol. Soc.* **106**, 85–100.

Wesely, M. L.: 1976, 'The Combined Effect of Temperature and Humidity Fluctuations on Refractive Index', *J. Appl. Meteorol.* **15**, 43–49.

Wilczak, J., Oncley, S., and Stage, S. A.: 2001, 'Sonic Anemometer Tilt Correction Algorithms', *Boundary-Layer Meteorol.* **99**, 127–150.

Wyngaard, J. C.: 1973, 'On Surface-Layer Turbulence', in: D. A. Haugen (ed.), *Workshop on Micrometeorology,* American Meteorological Society, Boston, Mass, pp. 101–149.

Wilson, K., Goldstein, A., Falge, E., Aubinet, M., Baldocchi, D., Berbigier, P., Bernhofer, C., Ceulemans, R., Dolman, H., and Field, C.: 2002, 'Energy Balance Closure at FLUXNET Sites', *Agric. For. Meteorol.* **113**, 223–243.